Sleep Medicine 14 (2013) 1112–1122

Contents lists available at ScienceDirect

Sleep Medicine

journal homepage: www.elsevier.com/locate/sleep

Original Article

How we fall asleep: regional and temporal differences in electroencephalographic synchronization at sleep onset

Cristina Marzano [a], Fabio Moroni [b], Maurizio Gorgoni [a], Lino Nobili [c], Michele Ferrara [d], Luigi De Gennaro [a,*]

[a] Department of Psychology, University of Rome "Sapienza", Rome, Italy
[b] Department of Psychology, University of Bologna, Bologna, Italy
[c] Centre of Epilepsy Surgery "C. Munari", Center of Sleep Medicine, Niguarda Hospital, Milan, Italy
[d] Department of Life, Health and Environmental Sciences, University of L'Aquila, Italy

ARTICLE INFO

Article history:
Received 4 February 2013
Received in revised form 15 May 2013
Accepted 21 May 2013
Available online 23 August 2013

Keywords:
Sleep onset
Theta oscillations
Occipital cortex
Anteroposterior changes
Oscillatory activity
EEG analysis
BOSC

ABSTRACT

Objectives: We hypothesized that the brain shows specific and predictable patterns of spatial and temporal differences during sleep onset (SO) reflecting a temporal uncoupling of electrical activity between different cortical regions and a dissociated wakelike and sleeplike electrocortical activity in different cortical areas.

Methods: We analyzed full-scalp electroencephalographic (EEG) recordings of 40 healthy subjects to investigate spatial and temporal changes of EEG activity across the wake-sleep transition. We quantified EEG sleep recordings by a fast Fourier transform (FFT) algorithm and by a better oscillation (BOSC) detection method to the EEG signals, which measured oscillatory activity within a signal containing a nonrhythmic portion.

Results: The most representative spatial change at SO is the frontalization of slow-wave activity (SWA), while the θ activity, which mostly shares a similar temporal and spatial pattern with SWA, exhibits a temporo-occipital diffusion. The time course of these oscillations confirms that the changes of the dominant waves coexist with topographic changes. The waking occipital prevalence of α oscillations is progressively replaced by an occipital prevalence of θ oscillations. On the other hand, more anterior areas show a wide synchronization pattern mainly expressed by slow waves just below 4 Hz and by spindle oscillations.

Conclusions: The whole pattern of results confirms that the centrofrontal areas showed an earlier synchronization (i.e., they fall asleep first). This finding implies a coexistence of wakelike and sleeplike electrical activity during sleep in different cortical areas. It also implies that the process of progressive brain disconnection from the external world as we fall asleep does not necessarily affect primary and higher-order cortices at the same time.

1. Introduction

A growing body of evidence strongly supports the notion that sleep is a local and use-dependent process. Multichannel electroencephalographic (EEG) recordings in humans indicate that practically every sleep phenomenon from sleep onset (SO) to the awakening is strictly local in nature [1]. Extensive regional differences have been documented at SO [2–5], across all-night nonrapid eye movement (NREM) and rapid eye movement (REM) sleep [6] and on awakening [7,8]. Similarly every sleep EEG rhythm occurs locally: slow oscillations (<1 Hz), slow waves (0.5–4 Hz), and sleep spindles (12–15 Hz) are local phenomena, as revealed by simultaneous EEG recordings of the scalp, intracerebral EEG recording [9], and unit firing in multiple brain regions of neurosurgical patients [10]. Additionally, θ (5–7 Hz) and α (8–11 Hz) oscillations in scalp recordings likewise are predominantly local [11].

In the spatial acceptation of the local sleep notion, we focused on the existence of topographic, frequency-specific EEG differences, which were stable within sleep states and within individuals. This interpretation encompasses phenomena such as the frontal prevalence of low-frequency oscillations during both NREM and REM sleep [6], explained by homeostatic sleep regulating processes that preferentially involve those neuronal populations which mostly have been activated during wakefulness [1], or like the individual centroparietal profile of the EEG activity in the 8- to 16-Hz frequency range during NREM sleep [12].

* Corresponding author. Address: Dipartimento di Psicologia – Sezione di Neuroscienze, Università di Roma "Sapienza," Via dei Marsi, 78, 00185 Roma, Italy. Tel.: +39 06 49917647; fax: +39 06 49917508.
E-mail address: luigi.degennaro@uniroma1.it (L. De Gennaro).

1389-9457/$ - see front matter © 2013 Elsevier B.V. All rights reserved.
http://dx.doi.org/10.1016/j.sleep.2013.05.021

Undoubtedly the transitions between states of vigilance and in particular SO are a privileged scenario in which local sleep processes do occur. EEG and corticographic recordings suggest that SO is characterized by massive regional brain heterogeneity. Low-frequency EEG activity is prominent at the more anterior areas, and >8 Hz frequencies are prevalent at the occipital regions during presleep wakefulness [4]. Then the α activity (8–12 Hz) spreads toward anterior areas, and the progressive synchronization of the EEG during NREM sleep is expressed by an increased centrofrontal prominence of low-frequency activity and by centroparietal maxima of the σ activity (12–14 Hz) [4]. Scalp observations have been supported by electrocorticographic recordings of epileptic patients undergoing presurgical assessment [13].

This orchestrated series of cortical changes seems to dynamically involve different areas and different EEG frequencies. As recently demonstrated in drug-resistant epileptic patients, widespread cortical territories can maintain an activated pattern for several minutes after the thalamic [14] and the hippocampal deactivation [15]. Interestingly, the thalamocortical delay in SO is highly variable between individuals and cortical projections, ranging from few seconds to more than 10 min [14]. Such temporal uncoupling of electrical activity between different cortical regions may result in the coexistence of wakelike and sleeplike electrical activity during sleep of different cortical areas [9].

Our study aimed to describe the local (cortical) specific patterns of EEG activity during SO. In particular, we analyzed full-scalp EEG recordings in a large sample of normal subjects to investigate spatial and temporal changes across the wakefulness to sleep transition. These local EEG changes during SO have been analyzed and quantified by a consolidated algorithm based on fast Fourier transform (FFT) algorithm and by a better oscillation (BOSC) detection method for the first time [11,16–18]. Therefore, we performed a single-Hz FFT investigation of spatial EEG changes at SO without any a priori assumption regarding the definition, the frequency-range, and the functional meaning of each EEG band. Then we assessed the temporal dynamics (time courses) of the classic EEG frequency bands before and after SO. Finally we investigated the changes across the wake-sleep transition by detecting EEG oscillations and then we analyzed their topographic differences and time courses.

2. Methods

2.1. Participants

Forty right-handed healthy subjects (20 men and 20 women) ages 18–29 years (mean age, 23.8 ± 2.88 years) were selected from a university student population. The inclusion criteria were normal sleep duration and schedule (habitual sleep time, 12:00 am–8:00 am ±1 h); no daytime nap habits; no excessive daytime sleepiness; and no other sleep, medical, neurologic, or psychiatric disorders, as assessed by a 1-week sleep log and by a clinical interview. Participants were required to avoid napping throughout the experiment; compliance was controlled by actigraphic recordings (AMI Mini Motionlogger).

All subjects gave their written informed consent. The study was approved by the Institutional Ethics Committee of the Department of Psychology of "Sapienza" University of Rome and was conducted in accordance with the Declaration of Helsinki.

2.2. Procedure

A dataset of a previous study was analyzed [19]. The sleep recordings were scheduled in the first night (adaptation), in the second night (baseline sleep), and in the fourth night (recovery sleep after 40 h of sleep deprivation). For the purposes of our study, only the second undisturbed baseline sleep night after the adaptation to laboratory sleep was considered.

Sleep recordings were performed in a soundproof temperature-controlled room. The subjects' sleep was undisturbed and started at midnight and ended after 7.5 h of accumulated sleep, as visually observed online by expert sleep researchers.

2.3. Polysomnographic recordings

An Esaote Biomedica VEGA 24 polygraph was used for polysomnographic (PSG) recordings. EEG signals were analogically filtered (high-pass filter at 0.50 Hz and antialiasing low-pass filter at 30 Hz [−30 dB/octave]). The 19 unipolar EEG derivations of the international 10–20 system (Fp1, Fp2, F7, F8, F3, F4, Fz, C3, C4, Cz, P3, P4, Pz, T3, T4, T5, T6, O1, O2) were recorded from scalp electrodes with averaged mastoid reference. The submental electromyogram (EMG) was recorded with a time constant of 0.03 s. Bipolar horizontal eye movements were recorded with a time constant of 1 second. The bipolar horizontal electrooculogram (EOG) was recorded from electrodes placed approximately 1 cm from the medial and lateral canthi of the dominant eye. Impedance of these electrodes was kept below 5 K Ohm.

2.4. Data analysis

2.4.1. PSG and quantitative analysis of EEG signals

Central EEG derivation (Cz), EMG, and EOG were used to visually score sleep stages in 12-second epochs, according to the standard criteria [20]. PSG measures provided a clear picture of a normal night sleep of adapted subjects (Table 1). It should be noted that sleep latency was characterized by a considerable variability between subjects (standard deviation, 11.43 min).

The polygraphic signals (19 EEG channels, EOG, and EMG) were converted online from analog to digital with a sampling rate of 128 Hz and stored on the disk of a personal computer. We investigated the 0.50- to 25.00-Hz frequency range, computing power spectra by a FFT routine for 4-second periodograms. Spectra from three consecutive 4-second epochs were averaged to allow alignment with the visual scoring of sleep stages, based on 12-second epochs. EEG topography was evaluated by comparing the 5-minute presleep vs. postsleep intervals. Ocular and muscle artifacts were carefully excluded offline by visual inspection. Due to the intrinsic characteristics of the presleep stage, the percentage of rejected 12-second epochs was higher in these 5-minute intervals (41.2% ± 16.4%) than in the postsleep intervals (21.0% ± 16.0%). Individual time series of EEG power values were aligned as a function of the first epoch of sleep defined on the basis of the appearance of the first k-complex or sleep spindle. In fact it has been previously demonstrated that the first epoch of stage 2 sleep represents an unequivocal hallmark for the beginning of sleep [21,22].

Data analysis was mostly performed with the software package MATLAB (The Math Works, Inc., MA, USA) and its signal analysis and statistics toolbox.

2.4.2. Single-Hz EEG topography

Before statistical analyses, the data were reduced to a 1-Hz bin width by collapsing four adjacent 0.25-Hz bins. The only exception was the 0.50- to 1.00-Hz bin, for which two adjacent 0.25-Hz bins were collapsed. The bins were referred to and plotted by the center frequency included in our study (e.g., the 2-Hz bin referred to the averaged values of the following bins: 2.00, 2.25, 2.50, and 2.75 Hz).

EEG power values for each 1-Hz frequency bin were considered as dependent measures and compared by paired t tests in the 5-minute intervals preceding and succeeding SO. Values were log

Table 1
Means and standard deviations of the polysomnographic variables.

	Mean	SD
SOL (min)	11.15	11.43
Presleep interval (min)	2.93	0.82
Postsleep interval (min)	3.95	0.80
Stage 1 (min)	27.95	12.94
Stage 2 (min)	262.33	40.69
SWS (min)	45.12	27.28
First NREM cycle (min)	65.66	15.86
REM (min)	105.99	21.43
WASO (min)	26.07	19.19
TST (min)	441.4	38.65
TBT (min)	484.8	63.93

Abbreviations: SD, standard deviation; SOL, sleep-onset latency; min, minutes; SWS, slow-wave sleep (stages 3 + 4); NREM, nonrapid eye movement sleep; REM, rapid eye movement sleep; WASO, wake after sleep onset; TST, total sleep time; TBT, total bed time.

transformed, color coded, plotted at the corresponding position on the planar projection of the scalp surface, and interpolated (biharmonic spline) between electrodes. The Bonferroni correction for multiple comparisons was applied. Considering the mean correlation between the variables ($r = 0.24$), the α level was then adjusted to $\leqslant .0005$ ($t \geqslant 3.82$).

2.4.3. Time course of EEG frequency bands

Due to the variable length of the presleep and postsleep intervals and of the first sleep cycle, we adopted the following procedure to make the individual time courses comparable: (1) the individual time courses were aligned as a function the first spindle or *k*-complex; (2) the time series of 12-second epochs during the presleep interval were divided into five segments, while the postsleep time series were divided into 20 segments (percentiles); and (3) we removed epochs with muscle, movement, or ocular artifacts and averaged individual time courses across subjects. This procedure strictly resembled that used for analyzing time courses of EEG changes during NREM and REM sleep, which usually are divided in 20 and 5 percentiles [23]. In this way, each pre- and postsleep interval represented a fifth and a 20th percentile of the total pre- and postsleep intervals, respectively. Neither skipped first REM sleep episodes nor SO REM sleep episodes were present in our recordings.

EEG power maps were computed for the following frequency EEG bands: δ (0.50–4.75 Hz), θ (5.00–7.75 Hz), α (8.00–11.75 Hz), σ (12.00–15.75 Hz), and β (16.00–24.75 Hz). These maps were calculated for the five time intervals preceding and following SO. To attempt to provide a synoptic description of the kinetics of EEG topography across the first sleep cycle, power maps at the 10th, 15th, and 20th time intervals also were calculated.

2.4.4. Detection of oscillatory activity

Because a spectral peak resulting from a FFT algorithm of the EEG signal does not necessarily imply an underlying oscillatory activity at that frequency, we also applied the BOSC detection method to the EEG signals. The BOSC is a method that was introduced by Caplan et al [16] and recently was applied to NREM and REM sleep recordings [11,18]; it is aimed to detect oscillatory activity within a signal containing a nonrhythmic portion. This method detects oscillatory activity in EEG signals by considering the functional form of the background nonrhythmic portion of the signal and revealing segments of the recording that significantly deviate from the spectral characteristics of the background.

The analysis was separately performed for each frequency of interest (in the 0.50–24.25-Hz range), electrode, and 5-minute time segment before and after SO. For a given frequency, an oscillatory episode was defined as an epoch longer than a duration threshold, D_T (set to three cycles in our analysis) during which wavelet power at frequency exceeded a power threshold (P_T). This P_T threshold was chosen as follows in the selected segments before and after SO: (1) the EEG was wavelet transformed (Morlet wavelet, window = 6 cycles) at 47 logarithmically spaced frequencies in the 0.50- to 24.25-Hz range. The average of the log-transform of these wavelet values yielded the wavelet power spectrum; and (2) the background noise spectrum assumed the form $\text{Power}(f) = Af^{-\alpha}$. The estimate of this background has been obtained by fitting the observed spectrum at each electrode with a linear regression in log to log units (see online Supplementary Figs. 1 and 2). The background at f^* has been estimated on the mean of its corresponding $\chi^2(2)$ probability distribution function. The power threshold (P_T) was set to the 95th percentile of the theoretical probability distribution. The proportion of time in which significant oscillations were detected before and after SO is termed $P_{episode}$ [24].

The BOSC method analysis was performed on the EEG signals recorded from each scalp location during the individual presleep and postsleep intervals and was averaged across subjects.

2.4.5. Time and spatial dynamics of oscillatory activity

To attempt to also provide a topographic description of the kinetics of detected oscillatory activity, the time course of the values of $P_{episode}$ resulting from five presleep and postsleep time intervals were reported for each frequency and scalp location.

2.4.6. Detection of oscillatory activity from a single patient with intracranial recording

As described in the Supplementary Material (see the online Supplementary Methods section), the BOSC detection method was applied to the stereo-EEG (SEEG) signals recorded from the right calcarine, the precuneus, and the third frontal gyrus cortices during a 5-minute period following SO.

3. Results

3.1. Single-Hz EEG topography

Power maps reported in Fig. 1 show profound differences between EEG activity before and after SO; these evident changes are largely substantiated by the statistical comparisons. The comparisons between EEG activity before vs. after SO were significant for all derivations ($P < .00005$) in the <8-Hz frequency range.

Low-frequency activity below 2 Hz was characterized by a relative prevalence of more anterior regions. This frontal prevalence was already visible before SO. The significant increase at SO involved practically the whole cortical areas, with maximal differences again in correspondence of the frontal areas. Maximal power values at 3–4 Hz showed a relatively slightly posterior prevalence over the central areas. Additionally, statistical differences pointed to more posterior maxima (parietal and occipital) at 4 Hz. This relative posteriorization became even more evident in the range of frequencies corresponding to the θ activity. The central sites showed maximal values of EEG power both before and after SO, but the largest change was shown by occipital sites at 5- to 7-Hz frequencies.

The topographic map of power values in the $\geqslant$8-Hz and $\leqslant$12-Hz range showed an inversion from a relatively posterior prevalence before SO to a relatively anterior prevalence after SO. The statistical comparisons showed significant increases for all the frontal and central sites (at 8, 11, and 12 Hz).

Power in the frequency range that corresponded to sleep spindles showed large differences in the maps before and after SO. By

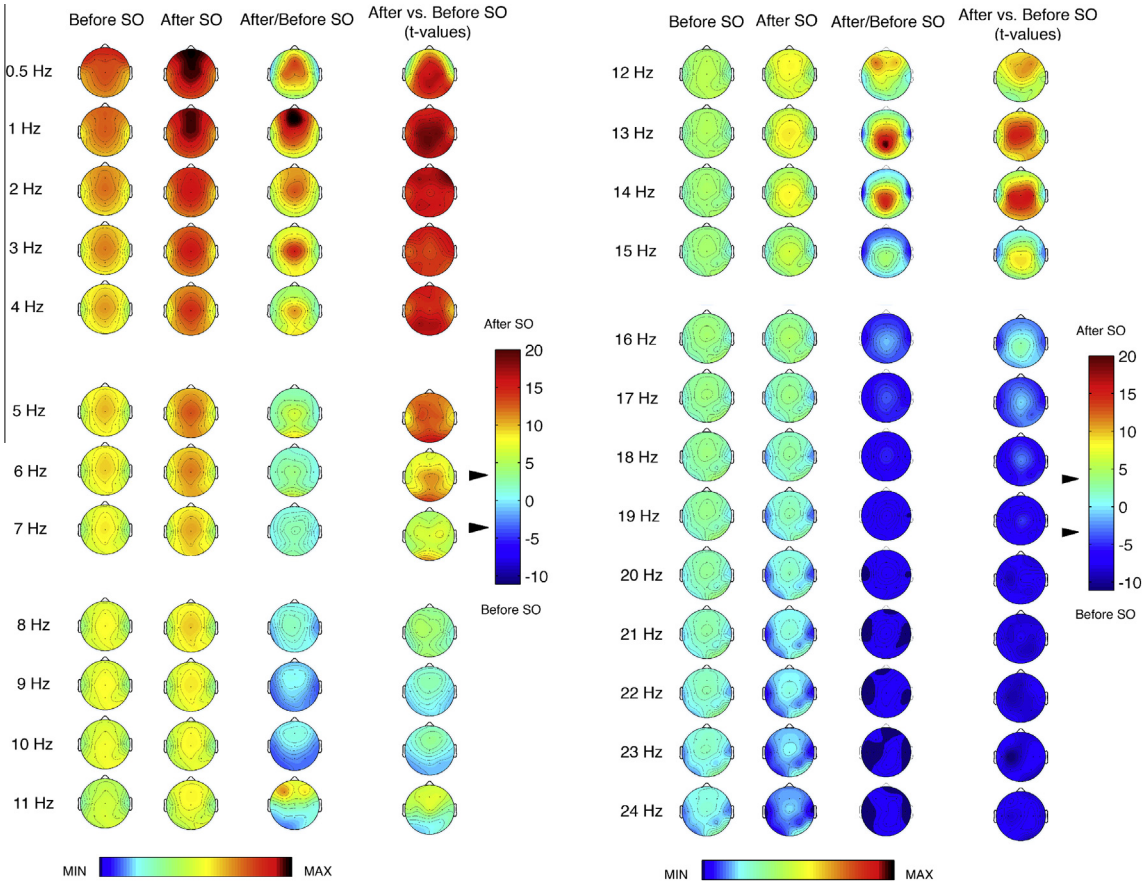

Fig. 1. Single-Hz electroencephalographic (EEG) topography (left side, frequency range = 0.50–11 Hz; right side, frequency range = 12–24 Hz). In both halves of the Fig., the first two columns show the topographic distribution of absolute EEG power in the 5-minute intervals preceding sleep onset (SO) (before SO) and those subsequent to SO (after SO), respectively. The maps were scaled between minimal (min) and maximal (max) values calculated for all frequencies and sites in before SO and after SO periods. The third column shows the relative EEG changes expressed as the ratio between after SO and before SO periods. The maps were scaled between min and max values in before SO and after SO periods. The fourth column shows the topographic statistical EEG power differences (assessed by paired t tests) between these 5-minute periods. Values are expressed in t test values: positive t test values indicate a prevalence of the after SO over the before SO period, and vice versa. The 2-tailed level of significance ($P \leqslant .000462$ after the Bonferroni test correction, corresponding to a $t \geqslant 3.82$) is indicated by the arrow in correspondence of the t test values color bar. Average values are normalized by total power; they are color coded and plotted at the corresponding position on the planar projection of the scalp surface and are interpolated (biharmonic spline) between electrodes. The maps are based on the 19 unipolar EEG derivations of the international 10–20 system with averaged mastoid reference. Maps are plotted for each frequency Hz bin in the 0.50- to 24.75-Hz range.

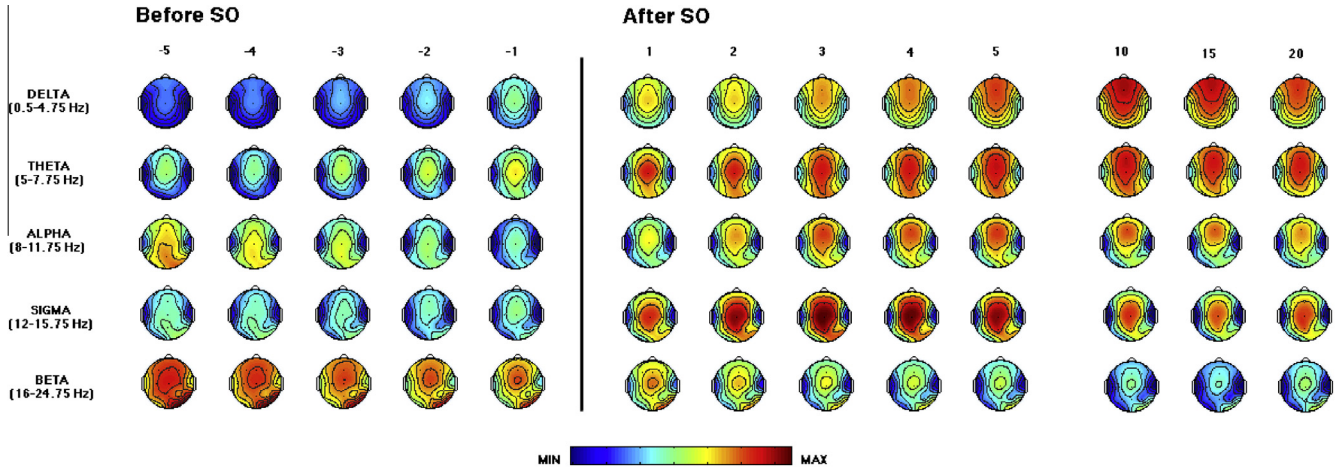

Fig. 2. Time course of electroencephalographic (EEG) frequency bands. From the left, topographic EEG shows changes across the interval preceding sleep onset (SO) (i.e., from the lights-off to the first epoch of sleep). The power maps obtained by subdividing the presleep interval into five equal parts (from the −fifth to −first). Data were calculated for each subject and then averaged across subjects. After the vertical line, indicating the first epoch of stage two, the first five intervals after SO (from the first–fifth) are plotted. The last three columns on the right side show power maps at the 10th, 15th, and 20th time intervals calculated across the first sleep cycle. Average values are normalized by total power; they are color coded and plotted at the corresponding position on the planar projection of the scalp surface and are interpolated (biharmonic spline) between electrodes. The maps are based on the 19 unipolar EEG derivations of the international 10–20 system with averaged mastoid reference. Maps are plotted for the following EEG bands: δ (0.50–4.75 Hz), θ (5.00–7.75 Hz), α (8.00–11.75 Hz), σ (12.00–15.75 Hz), and β (16.00–24.75 Hz).

definition this is a consequence of the scoring of SO as the first epoch of stage 2. The statistical comparisons at 13, 14, and 15 Hz clearly indicated that the maximal differences were located over the midsagittal centroparietal areas.

The 16-Hz bin stood as a watershed between the frequencies directly as an expression of the synchronized activity as consequences of SO, and as frequencies associated with a desynchronized activity of wakefulness. At 16 Hz, no regional difference was significant. The remaining 17- to 25-Hz range of EEG frequencies showed a widespread decrease of power after SO. Some frontal and temporal areas showed significant differences at 17 Hz. Interestingly the differences before vs. after SO were ever significant for all cortical areas after this frequency bin, without any clear regional prominence.

3.2. Time course of EEG frequency bands

Fig. 2 describes the evolution of the topographic EEG power changes across the SO point (i.e., across five equivalent time segments) and their temporal dynamics during the first NREM sleep episode. A buildup of the anteroposterior gradient of the slow-wave activity (SWA) with maximal power values over the midsagittal frontal pole was clearly visible. It reached its asymptote at the midpoint of the first sleep cycle (located in correspondence of the 10th interval, as the individual NREM episodes within the first sleep cycle were subdivided into 20 equal percentiles) and then decreased in proximity of the first REM episode (i.e., the time interval just before the 20th percentile). Before SO a low-level SWA already showed a relatively midsagittal centrofrontal prevalence, which largely increased after SO and attained the frontal prevalence at the third time segment.

To further characterize the temporal evolution of SWA across SO transition, the rise rate of SWA was modeled by a linear least-squares regression on individual data. The topographic distribution of the speed in the buildup of SWA confirmed an anteroposterior gradient of increasing sleep pressure (i.e., a faster buildup of SWA was associated to a higher homeostatic sleep pressure) [25], with a clear frontal prevalence (Fig. 3).

The θ activity showed steady centrofrontal prevalence across the presleep and postsleep intervals and during the whole first sleep episode. A relative increase of power in correspondence of occipital areas started just before SO, and it persisted across the whole sleep cycle. The α activity exhibited a janus bifrons nature, in which the occipital rhythm progressively decreased until the SO point; after this point, a centrofrontal activity began and reached the maximal power values over the frontal areas during the first sleep episode. A relatively low level of σ activity was discernible in the presleep intervals. As a consequence of the operational definition of SO, the σ activity (i.e., sleep spindles) immediately increased and took over its centroparietal localization.

As expected the β activity showed a progressive decrease from the interval before SO until the end of the sleep cycle. Its topography revealed a stable presleep and postsleep relative prevalence over central sites.

3.3. Detection and topography of oscillatory activity

As depicted by Fig. 4, which details EEG oscillations averaged across all the derivations, the EEG recordings of presleep wakefulness were dominated by the oscillations of the α waves, peaking at 9.85 Hz and secondarily by θ and β oscillations, peaking at 6.06 and 18.38 Hz, respectively (Fig. 5). The δ oscillations already were discernible in this averaged measure of oscillatory activity. After SO the EEG was dominated by spindle oscillations peaking at 13.00 Hz and by low-frequency oscillations in the range of δ and θ bands, peaking at 3.73 Hz and 6.06 Hz, respectively.

However, most of these oscillations were modulated by the scalp topography. The α waves in pre-SO EEG recordings and the θ waves of post-SO EEG recordings (Fig. 5) showed a marked occipital prominence. The δ oscillations in both presleep and postsleep EEG recordings had a relatively anterior prevalence (Fig. 5).

To provide a statistical assessment of these changes across the wake-sleep transition, we compared the proportion of time in

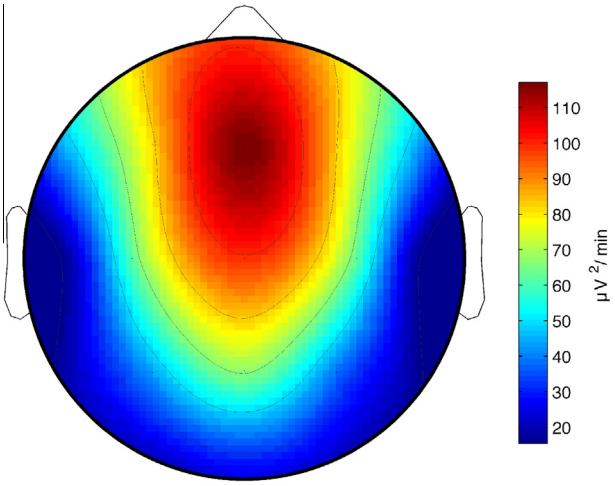

Fig. 3. Rise rate of slow-wave activity (SWA). Topographic distribution of the rise rate of SWA (0.50–4.75 Hz) during wake-sleep transition (i.e., five time intervals before and after sleep onset). The map is based on 19 electroencephalographic derivations, and values are color coded and plotted at the corresponding position on the planar projection of the hemispheric scalp model. Values between electrodes were linearly interpolated. The rise rate of SWA power was determined by linear regression on individual data. The regressions were significant for all derivations ($P < .05$).

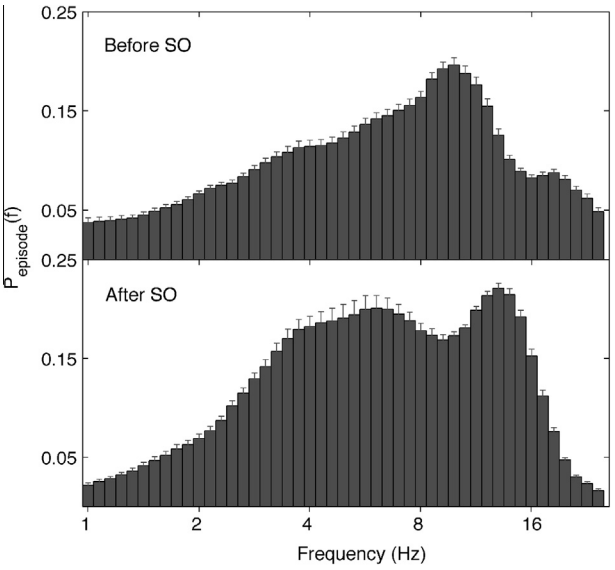

Fig. 4. Electroencephalographic (EEG) oscillations averaged across the whole derivations. The Fig. plots the mean proportion of time ($P_{episode}$ [f]) of the EEG before (upper panel) and after (lower panel) sleep onset in which oscillations were detected at each frequency. The detection of oscillations has been made by the better oscillation detection method (see Methods for details) on the 19 EEG electrodes. Error bars denote interlocation variability. Units of frequency are expressed in Hz and are plotted in 47 logarithmically spaced frequency values in the 0.50- to 24.25-Hz frequency range.

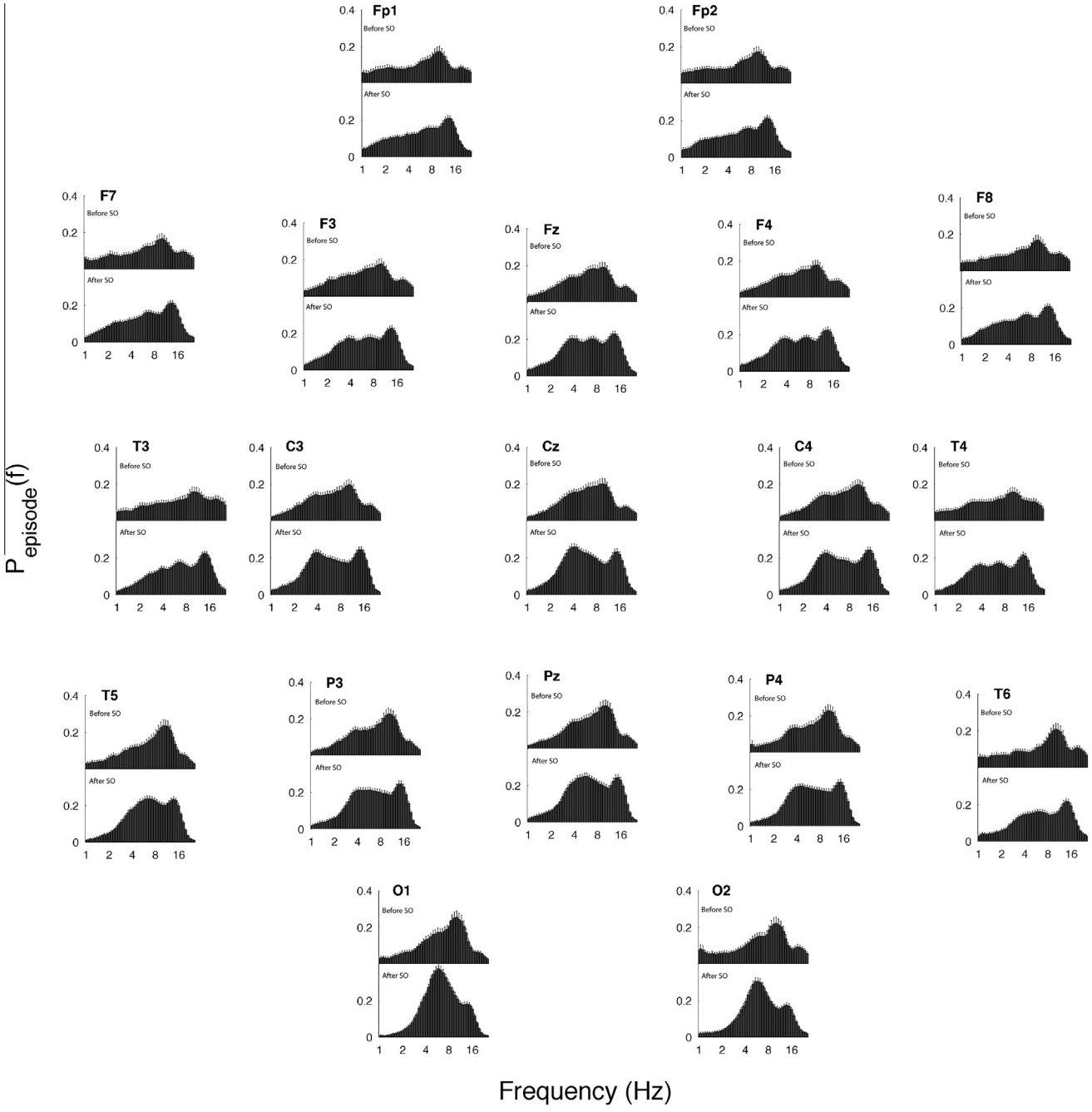

Fig. 5. Topographic distribution of electroencephalographic (EEG) oscillations detected by the better oscillation method during the 5-minute time segments before and after sleep onset (SO) (upper and lower panels, respectively). The mean proportion of time ($P_{episode}$ [f]) of the EEG before and after SO in which oscillations were detected for each scalp location is plotted. Error bars denote intersubject variability. Units of frequency are expressed in Hz and are plotted in 47 logarithmically spaced frequency values in the 0.50- to 24.25-Hz frequency range.

which significant oscillations were detected within the pre-SO and post-SO intervals between derivations, limited to the frequency peak of each band (Fig. 6). The δ oscillations increased after SO with maximal values at the vertex, and this increase was significant for the whole scalp locations. The θ oscillations largely increased after SO, with significant changes across all the derivations but a notable exception of most of the frontal areas. The magnitude of this increase was much greater over occipital areas and secondarily over temporal areas. The α oscillations did not show any significant difference when comparing the presleep vs. postsleep intervals. A different picture was provided by the spindle oscillations, which significantly increased after SO compared to the interval before SO over all the scalp locations, with the exception of the occipital areas. More importantly, the comparisons depicted a univocal anteroposterior gradient with the largest difference at the vertex. Finally β oscillations significantly decreased in laterofrontal sites and in the right occipital area after SO.

3.4. Time course of oscillatory activity

Fig. 7 shows the topographic time course of the oscillatory activity in the 0.50- to 24.25-Hz frequency range during the SO interval. The temporal dynamics of oscillatory activity during the wake-sleep transition pointed to a relative prevalence of α oscillations in the first time segments of presleep wakefulness. Just before SO, α oscillations were mostly replaced by θ oscillations.

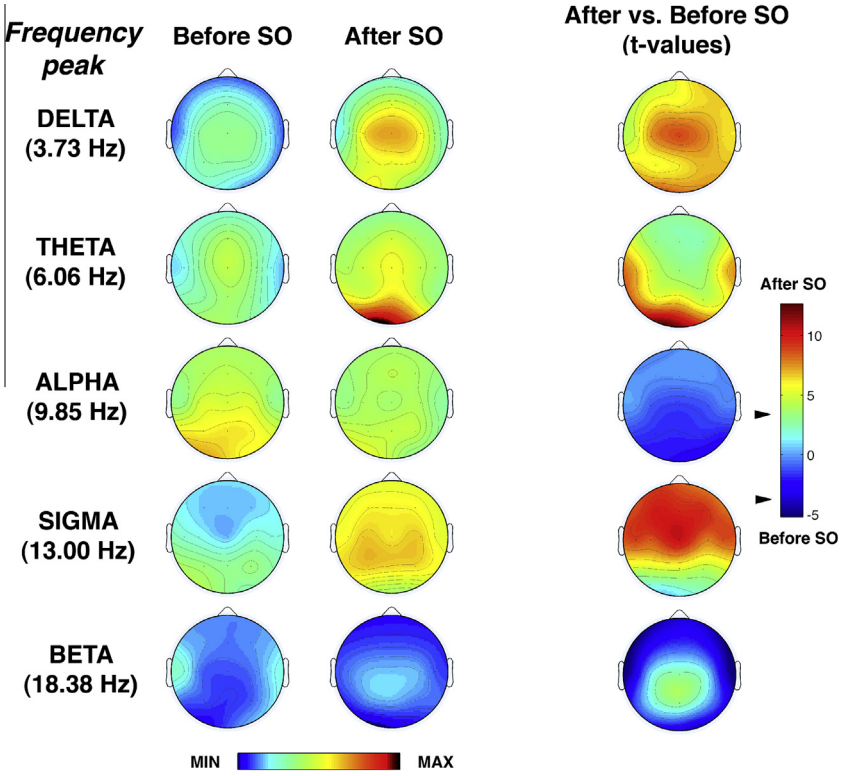

Fig. 6. Topographic distribution of the frequency peak of oscillatory activity within each electroencephalographic (EEG) frequency bands. From the left, the first two columns show the topographic distribution of the mean proportion of time in which oscillations were detected ($P_{episode}$) in correspondence of five selected frequencies of interest (3.73, 6.60, 9.85, 13.00, 18.38 Hz) among the five frequency bands (δ, θ, α, σ, β) in the 5-minute intervals preceding sleep onset (SO) (before SO) and subsequent to SO (after SO), respectively. The maps were scaled between minimal (min) and maximal (max) values in the before SO and after SO periods. The first column on the right side shows topographic statistical $P_{episode}$ differences (assessed by paired t tests) between after SO and before SO periods. Values are expressed in t values: positive t values indicate a prevalence of the after SO over the before SO period, and vice versa. The 2-tailed level of significance ($P \leqslant .00087$ after the Bonferroni correction, corresponding to a $t \geqslant 3.61$) is indicated by the arrow in correspondence of the t values color bar. Average values are normalized by total power; they are color coded and plotted at the corresponding position on the planar projection of the scalp surface and are interpolated (biharmonic spline) between electrodes. The maps are based on the 19 unipolar EEG derivations of the international 10–20 system with averaged mastoid reference.

Then EEG recordings showed a massive synchronization pattern within the frequency ranges of the δ, θ, and spindles oscillations. However, this general dynamic was different for some specific areas, according to a general anteroposterior gradient.

Over the occipital regions, α oscillations, which dominated the pre-SO interval, were gradually replaced by slower oscillations within the θ range; θ oscillations strongly increased after SO and they dominated the entire sleep period. Although present, a low proportion of δ and spindle oscillations were extracted during this time window. A similar dynamic was still discernible over the parietal regions, but δ waves progressively became the dominant oscillations after SO according to an anteroposterior gradient. This finding was even more evident when moving from the central areas to the frontal ones.

Spindle oscillations became progressively more intense as a function of time from SO, and they affected a wide part a scalp, including the frontal, central, and parietal regions. The α oscillations characterized the early intervals of the transition with maximal parieto-occipital values. Then they reappeared in the late intervals after SO, with a relatively more anterior localization. The β oscillations progressively disappeared as SO continued with maximal values in the early phase of the presleep interval over temporofrontal lateral areas.

4. Discussion

We described an orchestrated series of changes which dynamically involved the different cortical areas and different EEG frequencies when we fall asleep. Undoubtedly EEG synchronization was the most representative change of SO. It was expressed by significant increases of low-frequency activity which involved all cortical areas within the range of 0.50–7 Hz. The subsequent range (from 8–12 Hz), which encompasses the classical α rhythm, confirms the inversion from an occipital prominence of presleep wakefulness to an anterior prevalence after SO [4]. EEG power in the frequency range corresponding to sleep spindles showed maximal differences over the midsagittal centroparietal areas, and these changes coincided with the consolidated topography of sleep spindles [26]. As a mirror image of the low-frequency activity increased, SO was characterized by a decrease in the 18- to 25-Hz activity, significantly over all the cortical areas and without a clear regional prevalence.

These spatial changes evolved over the time segment, and the frontalization of SWA was associated with a faster buildup of homeostatic sleep pressure, as expressed by the rise rate of SWA during SO. At the same time the θ activity, which mostly shared a similar temporal and spatial pattern with SWA, also exhibited an occipital diffusion. The current application of a method to detect rhythmic oscillations in EEG recordings strengthens these results, and the BOSC analysis confirms and extends most of the results based on FFT analyses. The evolution of these oscillations in the wake-sleep transition period confirms that the changes of the dominant rhythms coexist with topographic changes. In particular, there was a shift from an occipital prevalence of α oscillations to a similar occipital prevalence of θ oscillations during SO. On the other hand, the more anterior areas showed a wide synchroniza-

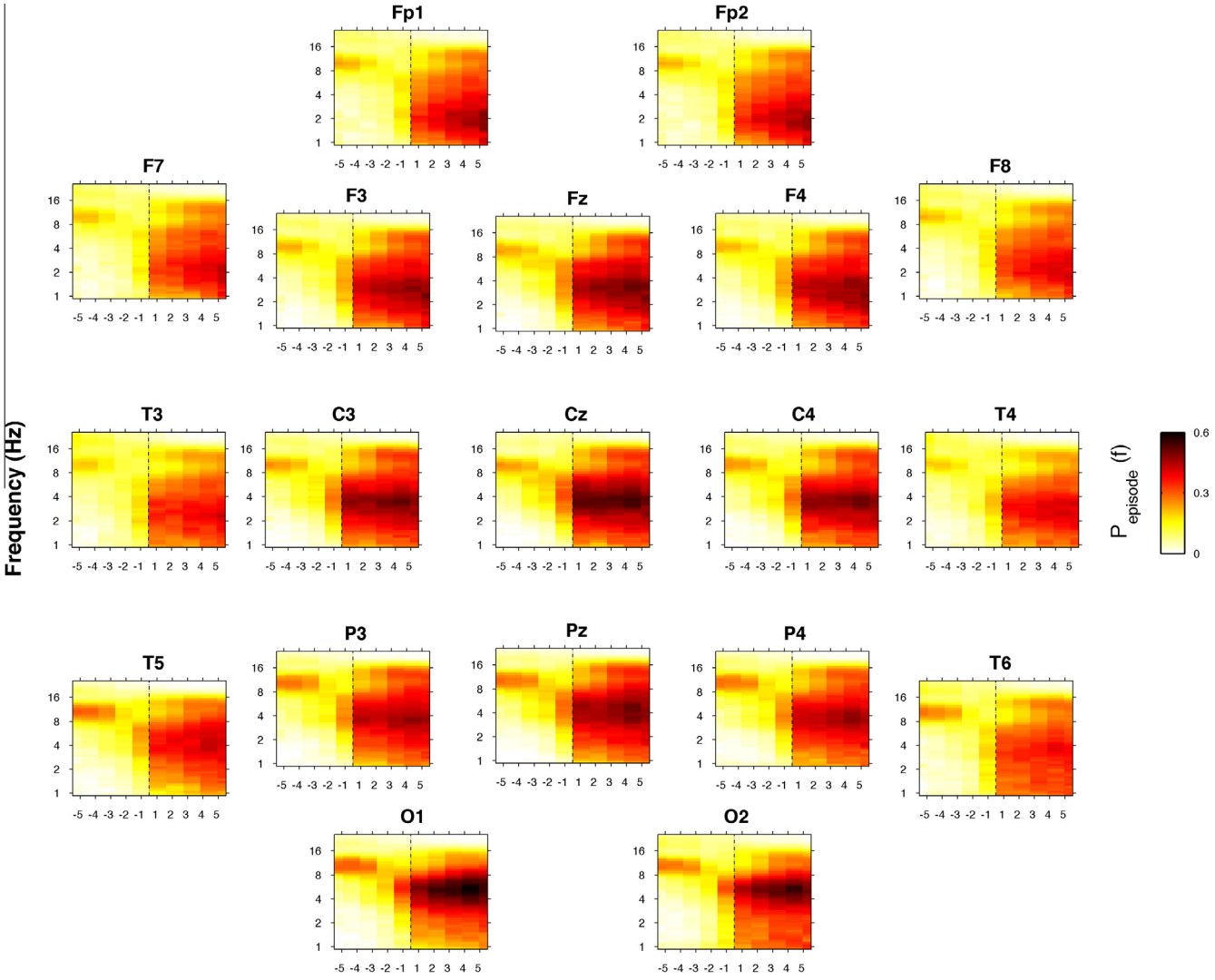

Fig. 7. Time course of oscillatory activity. Topographic time-frequency plots of the five intervals before (from the fifth–first) and after (from the first–fifth) SO, averaged across subjects at the 19 scalp derivations. The presleep and postsleep intervals were divided into five equal parts as in Fig. 2. Data were calculated for each subject and then were averaged across subjects. Darker colors (red brown) are indicative of increased oscillatory ($P_{episode}$) activity for a specific frequency of oscillation in the 0.50- to 24.25-Hz frequency range. SO is indicated by a black dotted line. (For interpretation of the references to colour in this figure legend, the reader is referred to the web version of this article.)

tion pattern mainly expressed by slow waves just below 4 Hz and by spindle oscillations.

It should be noted that no <1 Hz slow oscillations after SO have been detected by the BOSC method, while relatively high power values have been found by the FFT analysis. This finding should be reasonably explained by the duration threshold, D_T, of the BOSC algorithm, which is set to 3 cycles to eliminate artifacts and non-rhythmic oscillations [16,17]. This threshold might be conservative for these slow oscillations.

4.1. The anteriorization of SWS

Our results once more confirm that centrofrontal areas show an earlier and stronger electrophysiologic synchronization [4–6]. However, this pattern of synchronization does not strictly include θ and α oscillations, as their topographic and temporal characteristics seem different. When we first reported the existence of regional asynchronies in the SO process [4], we were driven by a general aim of a simplification of the EEG rhythms during the wake-sleep transition. This simplification was mainly prompted by the cellular observations on the mechanisms underlying these EEG waves by Steriade [27], aimed at reducing the multiplicity of the EEG rhythms to a few basic cellular operations of the thalamocortical machine. At that time, a generalized increase of EEG activity across the 1- to 15-Hz frequency range with an anteroposterior gradient was the most parsimonious conclusion based on our findings, limited to 4 scalp locations and to a procedure of principal component analysis to group single-Hz EEG frequencies.

Our results suggest the existence of less simplified mechanisms. The anteroposterior gradient still suggested an earlier and more pronounced synchronization of the anterior areas compared to sensory cortices. This finding also is associated to a steeper buildup of SWA, which indicated a higher homeostatic sleep pressure [25], and is coherent with the notion that slow waves propagate from prefrontal cortex toward posterior regions [5,10].

Finally, it should be noted that a relative increase of δ activity also is discernible before SO, and this finding implies that the standard PSG criteria may overestimate sleep latency, as intervals of EEG containing δ activity might be not detected by visual scoring.

4.2. The θ oscillations and SO of occipital areas

After the pioneering observations by Wright et al [3] in 1995, who first suggested a posterior increase of θ power from the first to the last minute of stage 1 sleep, Finelli et al [28] reported a maximum of θ activity in the parietooccipital region (secondary to a primary anterior predominance) in the recovery night after 36 h of prolonged wakefulness. A similar secondary peak (as compared to a primary frontal prominence) of significant increase of θ activity also has been observed in the waking EEG after 40 hours of sleep deprivation [29]. This converging evidence suggests that the occipital θ activity is associated to physiologic states having a high sleep pressure in common: sleep deprivation, recovery sleep, and SO. Our findings on the detection of θ oscillations and on their time course further strengthen this notion. Although most cortical regions progressively increase the δ oscillations with a marked prominence of centrofrontal areas and progressively increase spindle oscillations with a relative prevalence of centroparietal areas, occipital and temporo-occipital regions are dominated by the θ oscillations.

Based on these findings, we had the opportunity to analyze simultaneous intracerebral neocortical recordings of occipital (calcarine cortex), parietal (precuneus), and frontal (third frontal gyrus) cortices in one female patient with refractory epilepsy for an interval of 5 min after SO to explore the possibility that scalp θ activity and θ oscillations corresponded to an intrinsic oscillatory activity of the occipital cortex during the wake-sleep transition. We applied the BOSC analysis to these recordings, and we observed that the θ oscillation was the main oscillatory activity of the calcarine cortex, while the parietal and frontal regions showed δ, spindle, and β oscillations (see online Supplementary Material, Fig. 3). Hence it is likely that findings on the scalp EEG recordings were the expression of the local peculiar electrophysiology of the calcarine cortex.

Interestingly while reviewing neuroimaging studies of the waking-sleep transition, we were surprised to retrieve univocal results in the metabolic changes in visual areas at SO. Kjaer et al [30] measured regional cerebral blood flow by using $H_2{}^{15}O$-PET and found increases in extrastriate areas and decreases in posterior parietal (precuneus) and frontal (premotor) cortex. Cerebral blood flow velocity over occipital areas increases at the α–θ transition [31], different from the long-term reduction associated with stable NREM sleep [32,33]. Fukunaga et al [34] showed a higher amplitude (up to 1.71%) of blood oxygenation level–dependent functional magnetic resonance imaging signal fluctuation in visual cortex in subjects who just fell asleep compared to presleep wakefulness. In light sleep, significant increases in the fluctuation level of the blood oxygenation level–dependent signal also were observed in several cortical areas, among which visual cortex was the most significant [35] in the occipital cortex [36] and in the dorsal attention network [37].

These unexpected findings have been tentatively interpreted as reflecting a persistence of the default mode network during light sleep [35,37] or the electrophysiologic correlate of mental imagery continuing during sleep in the form of dreamlike mentation [34] or visual-hallucinatory hypnagogic activity [35].

We have no empirical evidence to disentangle between these two interpretations, though they do not seem to be mutually exclusive. On the one hand, the progressive increase of θ oscillations over the occipital and temporo-occipital regions may be associated to metabolic increases in these areas. On the other hand, increases of θ oscillations after SO also may be implicated in the formation of episodic memories. In fact a large body of experimental evidence relates encoding of episodic information to local θ oscillations both during wakefulness [38–43] and during sleep when it is associated to a successful dream recall [11]. Both findings seem more coherent with an association with a cognitive functioning specific to this transition state (i.e., hypnagogic visual imagery).

4.3. The α waves in wakefulness and sleep

At the start of the presleep interval, α activity is higher in correspondence of the occipital sites and it gradually decreases until SO. Then it progressively increases with centrofrontal maxima across the first sleep episode. This time course mostly replicates previous findings, which suggested a change of functional meaning of this rhythm from wakefulness to sleep [4,44,45]. However, the detection of EEG oscillations and their time course do not confirm the existence of an oscillatory activity in this frequency range after SO. Actually this is one of the few instances in which FFT and BOSC analyses point to different results. At least in the selected interval, it should be considered a nonrhythmic background activity.

It should be noted that we have discussed and named the 8- to 12-Hz power as "α" activity, which has been done due to the fact that this frequency range unequivocally corresponds to the α rhythm during wakefulness (i.e., during the presleep period). The same notation has been maintained after SO for congruency and also because we think that the <12-Hz range does not identify a different (independent) EEG rhythm (e.g., the so-called slow spindles). In fact electrophysiologic studies have attributed the whole frequency range of sleep spindles to a single mechanism, namely the duration of the hyperpolarization-rebound sequence in thalamocortical neurons, with long hyperpolarizations generating slower EEG frequencies and short hyperpolarizations yielding faster EEG frequencies [e.g., 46]. Furthermore, the cortical areas on which slow spindles have been detected are related to those thalamic nuclei in which relay cells display long hyperpolarizations [Steriade, personal communication]. Coherent with these observations, intracranial EEG recordings in humans show that >12-Hz EEG activity temporally precedes 9- to 12-Hz activity [47]. We also have found that the analysis of individual EEG topography points to only one kind of sleep spindle, peaking within the 12.25- to 13.75-Hz frequency and that regional, intranight, and homeostatic changes similarly affect the broader frequency range starting from 8 Hz [12]. Another recent intracranial EEG study refuted the concept of two distinct thalamocortical circuitries generating two types of spindles and rather suggests a continuous rostrocaudal change of spindle frequencies, which reflects the existence of different thalamocortical circuits and their modulation by corticothalamic and corticocortical connections [48]. Finally the current lack of a rhythmic activity in this range after SO detected by our BOSC analysis also is coherent with this interpretation.

4.4. Spindle oscillations and the decrease of β activity after SO

The σ activity already appears as spindle oscillations in the first minutes after SO. This finding seems coherent with recent intracranial findings, which have shown that faster (>12.5 Hz) centroparietal σ activity precedes slower (from 11.5 to 10.4 Hz) frontal EEG activity [49]. Similarly concurrent recordings of magnetoencephalography (MEG) and EEG have shown that MEG spindles largely occur without EEG spindle, while EEG spindles rarely occur without MEG spindles [49]. This observation has been interpreted in the differences of basic circuitry with an earlier activation of the substrate of MEG spindles, which may lead to activate the neural substrate of EEG spindles [49]. A possible explanation for these and our findings is that >12-Hz and <12-Hz EEG activity arise at different hyperpolarization levels of thalamocortical neurons (see above) and that different thalamic nuclei project to different cortical regions (i.e., posterior and lateral dorsal nuclei project to centroparietal cortex, whereas ventral and anterior dorsal nuclei

mainly project to prefrontal regions) [50,51]. Then these locations may recruit other areas, especially the frontal cortex, until a critical mass is achieved and it results in a diffuse generation of EEG spindles [49].

Compared to the presleep interval, the EEG after SO also is characterized by a generalized decrease of β activity power over almost all scalp locations, with a maximum over temporal areas. This pattern of changes confirms and extends previous findings of a progressive decrease of fast frequencies activity across SO period [22,52]. The findings also are coherent with the hyperarousal model of sleep initiation difficulties, as indexed by increased β EEG activity in individuals with insomnia [53,54]. In fact this neurocognitive model is based on the observation that cortical arousal, as indexed by high β activity, is enhanced in insomnia at or around SO and may be maintained as a result of classical conditioning. Moreover, because cortical EEG signals more often are affected by the electrical activity of the muscle tissue in the temporal sites on the skull [55], the decrease of β activity in the lateral temporal areas after SO might represent a reduction of muscular tone, which actually characterizes the beginning of stage 2.

As a final note of caution, it should be mentioned that our conservative choice to remove 12-second epochs containing artifacts and slow eye movements before the FFT analyses led to a higher percentage of rejected epochs in the presleep interval. Notably the actual percentage of rejected epochs strictly coincided with that found in our previous study on the wake-sleep transition, in which we used the same method [22]. This method might have affected the temporal continuity of the falling asleep process. However, we decided to divide the time series of the presleep and postsleep intervals into 5 and 20 percentiles at variance with that study by using the procedure commonly used for analyzing the time course of EEG changes during NREM and REM sleep [23]. This method has been done to compare time courses of different lengths and with different percentages of rejected epochs. We are aware that this procedure does not make equivalent presleep and postsleep intervals, though it makes these time courses comparable between subjects under the assumption that the interest is devoted to describe the time evolution of sleep changes.

5. Conclusion

Our brain shows striking spatial (local) differences in the specific patterns of EEG power and oscillatory activity when we fall asleep, with peculiar time courses at different locations over the scalp. Our results confirm that centrofrontal areas show an earlier and higher electrophysiologic synchronization/deactivation (fall asleep first and need more sleep). This finding implies that sleep features may appear in some cortical areas, while other neural networks maintain relatively high levels of activation. There is indeed recent evidence of unchanged or modest increases of functional connectivity in sensory (visual, auditory, and somatomotor) and cognitive networks (e.g., dorsal attention, default and executive control) at SO [37]. In this view, it does not seem surprising that 50% of normal sleepers report being awake if awakened at the first sleep spindle of the night [56], 55% of all PSG stage 2 sleep is judged to be periods of wakefulness [57], and 10% of subjects reaching stage 2 sleep report not falling asleep at all during a 45-minute nap period [56]. This misperception is even higher in insomniacs, and it becomes pathognomonic of paradoxical insomnia [58,59]. In our view, the time is mature for studying the neural mechanisms of perception of sleep in insomnia and normal sleep, and our results may be a starting point for novel investigations with a potentially high clinical relevance.

Conflict of interest

The ICMJE Uniform Disclosure Form for Potential Conflicts of Interest associated with this article can be viewed by clicking on the following link: http://dx.doi.org/10.1016/j.sleep.2013.05.021.

Acknowledgements

Our work was supported by grants from the Compagnia di San Paolo, Programma Neuroscienze 2008/09 (3889 SD/sd, 2008.1300) and from the Ministero Salute Ricerca Finalizzata 2009 (RF-2009-1528677) to L.D.G., and a grant from the Fondazione del Monte di Bologna e Ravenna to F.M.

We thank Benedetta Marino for her help in data collecting.

Appendix A. Supplementary data

Supplementary data associated with this article can be found, in the online version, at http://dx.doi.org/10.1016/j.sleep.2013.05.021.

References

[1] Ferrara M, De Gennaro L. Going local: Insights from EEG and stereo-EEG studies of the human sleep-wake cycle. Curr Top Med Chem 2011;11:2423–7.
[2] Broughton R, Hasan J. Quantitative topographic electroencephalographic mapping during drowsiness and sleep onset. J Clin Neurophysiol 1995;12:372–86.
[3] Wright KP, Badia P, Wauquier A. Topographical and temporal patterns of brain activity during the transition from wakefulness to sleep. Sleep 1995;18:880–9.
[4] De Gennaro L, Ferrara M, Curcio G, Cristiani R. Antero-posterior EEG changes during the wakefulness-sleep transition. Clin Neurophysiol 2001;112:1901–11.
[5] Massimini M, Huber R, Ferrarelli F, Hill S, Tononi G. The sleep slow oscillation as a traveling wave. J Neurosci 2004;24:6862–70.
[6] Marzano C, Ferrara M, Curcio G, De Gennaro L. The effects of sleep deprivation in humans: Topographical electroencephalographic changes in NREM versus REM sleep. J Sleep Res 2010;19:260–8.
[7] Ferrara M, Curcio G, Fratello F, Moroni F, Marzano C, Pellicciari MC, et al. The electroencephalographic substratum of the awakening. Behav Brain Res 2006;167:237–44.
[8] Marzano C, Ferrara M, Moroni F, De Gennaro L. Electroencephalographic sleep inertia of the awakening brain. Neuroscience 2011;176:308–17.
[9] Nobili L, Ferrara M, Moroni F, De Gennaro L. Lo Russo G, Campus C, et al. Dissociated wake-like and sleep-like electro-cortical activity during sleep. Neuroimage 2011;58:612–9.
[10] Nir Y, Staba RJ, Andrillon T, Vyazovskiy VV, Cirelli C, Fried I, et al. Regional Slow Waves and Spindles in Human Sleep. Neuron 2011;70:153–69.
[11] Marzano C, Ferrara M, Mauro F, Moroni F, Gorgoni M, Tempesta D, et al. Recalling and forgetting dreams: Theta and alpha oscillations during sleep predict subsequent dream recall. J Neurosci 2011;3:6674–83.
[12] De Gennaro L, Ferrara M, Vecchio F, Curcio G, Bertini M. An electroencephalographic fingerprint of human sleep. Neuroimage 2005;26:114–22.
[13] Bódizs R, Sverteczki M, Lázár AS, Halász P. Human parahippocampal activity: non-REM and REM elements in wake-sleep transition. Brain Res Bull 2005;65:169–76.
[14] Magnin M, Rey M, Bastuji H, Guillemant P, Mauguiere F, Garcia-Larrea L. Thalamic deactivation at sleep onset precedes that of the cerebral cortex in humans. Proc Natl Acad Sci USA 2010;107:3829–33.
[15] Nobili L, De Gennaro L, Proserpio P, Moroni F, Sarasso S, Pigorini A, et al. Local aspects of sleep: Observations from intracerebral recordings in humans. Prog Brain Res 2012;199:219–32.
[16] Caplan JB, Madsen JR, Raghavachari S, Kahana MJ. Distinct patterns of brain oscillations underlie two basic parameters of human maze learning. J Neurophysiol 2001;86:368–80.
[17] Whitten TA, Hughes AM, Dickson CT, Caplan JB. A better oscillation detection method robustly extracts EEG rhythms across brain state changes: the human alpha rhythm as a test case. Neuroimage 2011;54:860–74.
[18] Moroni F, Nobili L, De Carli F, Massimini M, Francione S, Marzano C, et al. Slow EEG rhythms and inter-hemispheric synchronization across sleep and wakefulness in the human hippocampus. Neuroimage 2012;60:497–504.
[19] De Gennaro L, Marzano C, Fratello F, Moroni F, Pellicciari MC, Ferlazzo F, et al. The EEG fingerprint of sleep is genetically determined: A twin study. Ann Neurol 2008;64:455–60.
[20] Rechtschaffen A, Kales A, editors. A Manual of Standardized Terminology, Techniques and Scoring System for Sleep Stages of Human Subjects. Los Angeles, CA: UCLA Brain Information Service; 1968.

[21] De Gennaro L, Ferrara M, Ferlazzo F, Bertini M. Slow eye movements and EEG power spectra during wakefulness-sleep transition. Clin Neurophysiol 2000;111:3007–15.
[22] De Gennaro L, Ferrara M, Bertini M. The boundary between wakefulness and sleep: quantitative electroencephalographic changes during the sleep onset period. Neuroscience 2001;107:1–11.
[23] Aeschbach D, Borbély AA. All-night dynamics of the human sleep EEG. J Sleep Res 1993;2:70–81.
[24] Caplan JB, Glaholt MG. The roles of EEG oscillations in learning relational information. Neuroimage 2007;38:604–16.
[25] Finelli LA, Baumann H, Borbély AA, Achermann P. Dual electroencephalogram markers of human sleep homeostasis: correlation between theta activity in waking and slow-wave activity in sleep. Neuroscience 2000;101:523–9.
[26] De Gennaro L, Ferrara M. Sleep spindles: an overview. Sleep Med Rev 2003;7:423–40.
[27] Steriade M. Corticothalamic resonance, states of vigilance and mentation. Neuroscience 2000;101:243–76.
[28] Finelli LA, Achermann P, Borbély AA. Individual 'fingerprints' in human sleep EEG topography. Neuropsychopharmacology 2001;25:S57–62.
[29] De Gennaro L, Marzano C, Veniero D, Moroni F, Fratello F, Curcio G, et al. Neurophysiological correlates of sleepiness: a combined TMS and EEG study. Neuroimage 2007;36:1277–87.
[30] Kjaer TW, Law I, Wiltschiotz G, Paulson OB, Madsen PL. Regional cerebral blood flow during light sleep–a H(2)(15)OPET study. J Sleep Res 2002;11:201–7.
[31] Kotajima F, Meadows GE, Morrell MJ, Corfield DR. Cerebral blood flow changes associated with fluctuations in alpha and theta rhythm during sleep onset in humans. J Physiol 2005;568:305–13.
[32] Meadows GE, Dunroy HM, Morrell MJ, Corfield DR. Hypercapnic cerebral vascular reactivity is decreased, in humans, during sleep compared with wakefulness. J Appl Physiol 2003;94:2197–202.
[33] Meadows GE, O'Driscoll DM, Simonds AK, Morrell MJ, Corfield DR. Cerebral blood flow response to isocapnic hypoxia during slow-wave sleep and wakefulness. J Appl Physiol 2004;97:1343–8.
[34] Fukunaga M, Horovitz SG, van Gelderen P, de Zwart JA, Jansma JM, Ikonomidou VN, et al. Large-amplitude, spatially correlated fluctuations in BOLD fMRI signals during extended rest and early sleep stages. Magn Reson Imaging 2006;24:979–92.
[35] Horovitz SG, Fukunaga M, de Zwart JA, van Gelderen P, Fulton SC, Balkin TJ, et al. Low frequency BOLD fluctuations during resting wakefulness and light sleep: a simultaneous EEG-fMRI study. Hum Brain Mapp 2008;29:671–82.
[36] Olbrich S, Mulert C, Karch S, Trenner M, Leicht G, Pogarell O, et al. EEG-vigilance and BOLD effect during simultaneous EEG/fMRI measurement. Neuroimage 2009;45:319–32.
[37] Larson-Prior LJ, Zempel JM, Nolan TS, Prior FW, Snyder AZ, Raichle ME. Cortical network functional connectivity in the descent to sleep. Proc Natl Acad Sci USA 2009;106:4489–94.
[38] Anderson KL, Rajagovindan R, Ghacibeh GA, Meador KJ, Ding M. Theta oscillations mediate interaction between prefrontal cortex and medial temporal lobe in human memory. Cer Cortex 2010;20:1604–12.
[39] Klimesch W, Doppelmayr M, Russegger H, Pachinger T. Theta band power in the human scalp EEG and the encoding of new information. Neuroreport 1996;7:1235–40.
[40] Osipova D, Takashima A, Oostenveld R, Fernandez G, Maris E, Jensen O. Theta and gamma oscillations predict encoding and retrieval of declarative memory. J Neurosci 2006;26:7523–31.
[41] Rutishauser U, Ross IB, Mamelak AN, Schuman EM. Human memory strength is predicted by theta-frequency phase-locking of single neurons. Nature 2010;464:903–7.
[42] Sederberg PB, Kahana MJ, Howard MW, Donner EJ, Madsen JR. Theta and gamma oscillations during encoding predict subsequent recall. J Neurosci 2003;23:10809–14.
[43] Weiss S, Rappelsberger P. Long-range EEG synchronization during word encoding correlates with successful memory performance. Cogn Brain Res 2000;9:299–312.
[44] Pivik RT, Harman K. A reconceptualization of EEG alpha activity as an index of arousal during sleep: all alpha activity is not equal. J Sleep Res 1995;4:131–7.
[45] De Gennaro L, Vecchio F, Ferrara M, Curcio G, Rossini PM, Babiloni C. Changes in fronto-posterior functional coupling at sleep onset in humans. J Sleep Res 2004;13:209–17.
[46] Steriade M, Amzica F. Coalescence of sleep rhythms and their chronology in corticothalamic networks. Sleep Res Online 1998;1:1–10.
[47] Andrillon T, Nir Y, Staba RJ, Ferrarelli F, Cirelli C, Tononi G, et al. Sleep spindles in humans: insights from intracranial EEG and unit recordings. J Neurosci 2011;31:17821–34.
[48] Peter-Derex L, Comte JC, Mauguière F, Salin PA. Density and frequency caudo-rostral gradients of sleep spindles recorded in the human cortex. Sleep 2012;35:69–79.
[49] Dehghani N, Cash SS, Halgren E. Emergence of synchronous EEG spindles from asynchronous MEG spindles. Hum Brain Mapp 2011;32:2217–27.
[50] Cappe C, Morel A, Barone P, Rouiller EM. The thalamocortical projection systems in primate: an anatomical support for multisensory and sensorimotor interplay. Cer Cortex 2009;19:2025–37.
[51] Zhang D, Snyder AZ, Shimony JS, Fox MD, Raichle ME. Noninvasive functional and structural connectivity mapping of the human thalamocortical system. Cer Cortex 2010;20:1187–94.
[52] Merica H, Gaillard JM. The EEG of the sleep onset period in insomnia: a discriminant analysis. Physiol Behav 1992;52:199–204.
[53] Perlis ML, Giles DE, Mendelson WB, Bootzin RR, Wyatt JK. Psychophysiological insomnia: the behavioural model and a neurocognitive perspective. J Sleep Res 1997;6:179–88.
[54] Perlis ML, Merica H, Smith MT, Giles DE. Beta EEG activity and insomnia. Sleep Med Rev 2001;5:365–76.
[55] Klass DW. The continuing challenge of artifacts in the EEG. Am J EEG Technol 1995;35:239–69.
[56] Bonnet MH, Moore SE. The threshold of sleep: perception of sleep as a function of time asleep and auditory threshold. Sleep 1982;5:267–76.
[57] Sewitch DE. The perceptual uncertainty of having slept: the inability to discriminate electroencephalographic sleep from wakefulness. Psychophysiology 1984;21:243–59.
[58] Edinger JD, Krystal AD. Subtyping primary insomnia: is sleep state misperception a distinct clinical entity? Sleep Med Rev 2003;7:203–14.
[59] Harvey AG, Tang NK. (Mis)perception of sleep in insomnia: a puzzle and a resolution. Psychol Bull 2012;138:77–101.